Journal Name

COMMUNICATION

Unprecedented coupling reaction between two anionic species of a closo -decahydrodecaborate cluster and an Anderson-type polyoxometalate

Received 00th January 20xx,
Accepted 00th January 20xx

DOI: 10.1039/x0xx00000x

www.rsc.org/

Manal Diab,[a,b] Ana Mateo,[c] Joumada Al Cheikh,[d] Mohamed Haouas,[a] Alireza Ranjbari, Flavien Bourdreux,[a] Daoud Naoufal,[b] Emmanuel Cadot,[a] Carles Bo,[c,d,*] Sébastien Floquet,[a,*]

Abstract. Two decahydrodecaborate-functionalized Anderson-Evans polyoxometalates have been synthesized. The compounds have been characterized in solution by ESI-MS, various NMR techniques and electrochemistry, while DFT calculation bring strong support to understand their properties.

Hydroborates constitute a wide family of clusters displaying properties in various domains,[1, 2] especially in medicine.[2-4] With this respect, due to the large neutron scatter cross section of ^{10}B atoms and the robustness and the non-toxicity of hydroborates in biological systems,[4] such compounds are very useful for cancer treatment, ~~known as~~ Boron Neutron Capture Therapy (BNCT). In particular, the clusters $[B_{10}H_{10}]^{2-}$ offer the possibility of various functionalizations[5] leading for instance to *closo*-decaborate-triethoxysilane which can be coordinated to luminescent dye doped silica nanoparticles, hence facilitating the tracing of the *closo*-decaborate drug pathway in BNCT.[6, 7] On their side, Polyoxometalates (POMs) constitute a highly versatile family of inorganic compounds, which can be finely tuned at the molecular level and can therefore display properties or applications in many domains of societal and environmental interests such as in biology or in medicine for instance, especially when organic groups or coordination complexes are associated to the POM architectures.[8-11] The elaboration of such hybrid functional POM-based molecules allows tuning their solubility, charge, electronic and electrochemical properties, as well as the capability to interact with biomolecules, membranes or proteins and finally allows to combine the properties of the POM with the properties of the appended subunit for the design of multifunctional devices.[12-14] Even if the functionalization of POMs by organic groups or complexes remains challenging, different strategies exist. The organotin or organosilyl derivatives of vacant polyoxotungstates as $PW_9O_{34}^{9-}$, $SiW_{10}O_{34}^{4-}$, $XW_{11}O_{39}^{7/8-}$ (X = P, Si), or $P_2W_{17}O_{61}^{10-}$, offer large diversities of compounds exhibiting a wide panel of applications,[12-14] while the Anderson-Evans type POMs of general formula $[H_y(XO_6)M_6O_{18}]^{n-}$, (y = 0–6, n = 2–8, M = Mo^{VI} or W^{VI}, and X = central heteroatom) constitute a very useful platform for the design of multifunctional hybrid POMs when the oxygen atoms of the central octahedron XO_6 can be replaced with tris-ligand ($(HOCH_2)_3CNH_2$) (Tris = tris(hydroxymethyl)aminomethane).[15, 16] Rompel and coworkers demonstrated that such hybrid molecular systems are capable of interacting with biological material.[17, 18] Therefore, driven by the biomedical applications which could be reached by associating hydroborates and Anderson-Evans POMs the aim of this study was to explore the synthetic routes for the elaboration of such novel hybrid systems. Karoui and Ritchie reported in 2016 the first examples of organoboron containing Anderson–Evans POMs[19] but in our case the synthetic challenge is to combine two anionic entities exhibiting two opposite redox characters.

Herein we report the coupling of the closo-decahydrodecaborate cluster with the tris-functionalized Al(III) and Mn(III) Anderson-Evans POMs giving the two novel functionalized hybrid POMs denoted hereafter **$AlMo_6$(TRIS-B_{10})** and **$MnMo_6$(TRIS-B_{10})$_2$**, which consist of Al and Mn-Anderson type POMs covalently linked to one and two $B_{10}H_9CO$ entities through the formation of amide functions. The syntheses of both compounds were led by post-functionalization of the literature-known tris-functionalized POMs $[AlMo_6O_{18}(OH)_3(TRIS)]^{3-}$ and $[Mn^{III}Mo_6O_{18}(TRIS)_2]^{3-}$,[20, 21] with the highly reactive cluster $[B_{10}H_9CO]^{-}$ [22] in presence of two equivalents of diisopropylethylamine (DIPEA) as base in dry acetonitrile at room

[a] Institut Lavoisier de Versailles, CNRS, UVSQ, Université Paris-Saclay, 45 av. des Etats-Unis, 78035 Versailles, France
E-mail: sebastien.floquet@uvsq.fr
[b] ~~Laboratory of Organometallic and coordination chemistry,~~ Laboratory of Inorganic and Organometallic Cooridiantion Chemistry LCIO, Lebanese University, Faculty of Sciences I, Hadath, Lebanon
[c] Institute of Chemical Research of Catalonia (ICIQ). The Barcelona Institute of Science and Technology. Av. Països Catalans 16, 43007 Tarragona (Spain)
[d] Departament de Química Física i Inorgànica, Universitat Rovirai Virgili, Marcelí Domingo s/n, 43007 Tarragona (Spain)
[e] Equipe de Recherche et Innovation en Electrochimie pour l'énergie (ERIEE), Institut de Chimie Moléculaire et des matériaux d'Orsay (ICMMO), UMR CNRS 8182, Université Paris-Sud, Université Paris-Saclay, 91405 Orsay, France.

Electronic Supplementary Information (ESI) available: Experimental section, FT-IR characterizations, ESI-MS spectra, additional NMR data, electronic spectra and additional cyclovoltamograms; additional data on DFT methods. Full computational results in ioChem-BD https://doi.org/10.19061/iochem-bd-1-136.

temperature under nitrogen to give the two compounds (see Supporting Information for more details). When stoichiometric ratios between POMs and (TBA)[$B_{10}H_9CO$] were used, powder corresponding to a mixture still containing 20% of the starting compound $[(AlMo_6O_{18})(TRIS)(OH)_3]^{3-}$ was obtained with Al, while it gave a mixture containing 80 % of $[(MnMo_6O_{18})(TRIS\text{-}B_{10})_2]^{7-}$ and 20% of $[(MnMo_6O_{18})(TRIS)(TRIS\text{-}B_{10})]^{5-}$ for Mn-Anderson POM. An excess of TBA[$B_{10}H_9CO$] was then introduced to reach the target products even if in the case of the Al-derivative POM we never succeed in getting powder with less than 10% of the starting precursor. Mixed salts of formulas $(TBA)_{3.5}(DIPEAH)_{3.5}[MnMo_6O_{18}(O_3C_4H_7NB_{10}H_9CO)_2]$ (**$MnMo_6(TRIS\text{-}B_{10})_2$**) and $\{[(TBA)_{3.5}(DIPEAH)_{1.5}(AlMo_6O_{18})(C_4H_7O_3NB_{10}H_9CO)(OH)_3]_{0.9}[(TBA)_3(AlMo_6O_{18})(C_4H_8O_3N)(OH)_3)]_{0.1}\}.5H_2O$ (**$AlMo_6(TRIS\text{-}B_{10})$**) were obtained.

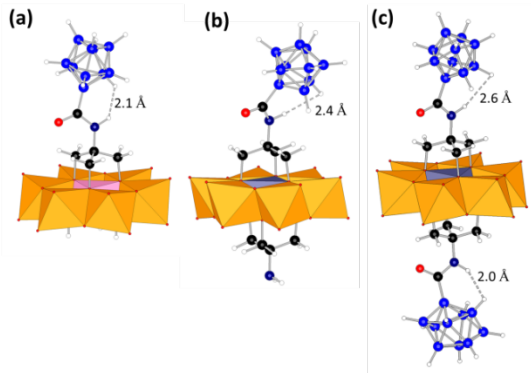

Figure 1. *DFT optimized structural models of* ***$AlMo_6(TRIS\text{-}B_{10})$*** *(a),* ***$MnMo_6(TRIS)(TRIS\text{-}B_{10})$*** *(b) and* ***$MnMo_6(TRIS\text{-}B_{10})_2$*** *(c). N in dark blue, B in blue, O in red, C in black, H in white, MoO_6 octahedra in orange, AlO_6 or MnO_6 octahedra in pink or in grey.*

The IR spectra of **$AlMo_6(TRIS\text{-}B_{10})$** and **$MnMo_6(TRIS\text{-}B_{10})_2$** (Figures S1-S2, ESI) feature characteristic vibrational bands of Anderson POMs between 900–940 cm^{-1} for the terminal Mo=O groups, and at 660 cm^{-1} for bridging Mo–O–Mo,[20, 23] while the disappearance of CO band at 2098 cm^{-1} typical of the carbonyl function in the $[B_{10}H_9CO]^-$ cluster is observed. Concomitantly, a new band assigned to the formation of an amide function –C(O)-NH- [7] is observed at 1588 cm^{-1} and the B-H vibration bands of the ~~hydro~~decaborate cluster appear shifted from 2517 cm^{-1} in $[B_{10}H_9CO]^-$ to 2473 cm^{-1}, which suggests the formation of dihydrogen contacts within the solids.[24] Taking molecular geometries (Figure 1) determined by means of a DFT based method (see ESI), the computed IR spectra of the two **$AlMo_6(TRIS\text{-}B_{10})$** and **$MnMo_6(TRIS\text{-}B_{10})_2$** compounds fully confirm the experimental findings. Number, location and intensity of bands agree nicely, although some computed peaks are slightly overestimated (Table S1, ESI).

Electrospray ionization mass spectrometry was applied to identify compounds **$AlMo_6(TRIS\text{-}B_{10})$** and **$MnMo_6(TRIS\text{-}B_{10})_2$**. The experiments performed in acetonitrile reveal several isotopic envelopes that are assigned as the anionic forms of **$AlMo_6(TRIS\text{-}B_{10})$**, $\{H_4AlMo_6O_{18}(OH)_3(O_3C_4H_7NB_{10}H_9CO).HCOOH.H_2O\}^{2-}$ at *m/z* 635.0 (calc *m/z* 634.8), $\{H_4AlMo_6O_{18}(OH)_3(O_3C_4H_7NB_{10}H_9CO)\}^-$, (m/z 1208.3, calc. m/z 1208.0) and a peak attributed to the di-anionic form of **$MnMo_6(TRIS\text{-}B_{10})_2$** as $\{[H_5MnMo_6O_{18}(O_3C_4H_7NB_{10}H_9CO)_2].CH_3CN.2H_2O\}^{2-}$ at *m/z* 763.4 (calc. *m/z* 763.6) for the second compound. See Figure S3-S5, ESI for more details.

Spectroscopic analysis of **$AlMo_6(TRIS\text{-}B_{10})$** and **$MnMo_6(TRIS\text{-}B_{10})_2$** using ^1H, ^{11}B, ^{13}C and ^{27}Al NMR in CD_3CN (Figures 2-3 and figures S6-S13, ESI) supports the formation of the target adducts. The $^{11}B\{^1H\}$ NMR spectra of **$MnMo_6(TRIS\text{-}B_{10})_2$** (Figure 2) and **$AlMo_6(TRIS\text{-}B_{10})$** (Figure S6) are very similar. The $^{11}B\{^1H\}$ NMR spectrum of TBA[$B_{10}H_9CO$] exhibits two signals at 5.1 and 6.1 ppm assigned to the two axial boron atoms of the cluster, four signals ranging from -17 to -31 ppm assigned to equatorial boron atoms and one signal at -44.4 ppm specific for the equatorial boron atom bearing the substituent CO. Upon reaction with $MnMo_6(TRIS)_2$ or $AlMo_6(TRIS)$ the signal at -44.4 ppm disappears for giving one signal around -25.0 ppm, typical of boron atom linked to an amide function {B-CO-NH-}.[7] Concomitantly, the signals of the apical boron atoms appeared overlapped at -0.5 ppm, while the signals of the equatorial boron atoms merge in a broader peak centered at -28.0 ppm. These results are rather consistent with the covalent linkage of the carbonyl function of $[B_{10}H_9CO]^-$ to the amine function of $MnMo_6(TRIS)_2$ and $AlMo_6(TRIS)$. For **$AlMo_6(TRIS\text{-}B_{10})$**, ^{27}Al NMR spectrum (Figure S8, ESI) exhibits only one peak centered at 16.41 ppm, which evidences that the $AlMo_6$ Anderson architecture is maintained. An additional minor peak (5-10 %) found at 13.5 ppm is also observed and could be attributed to starting POM accordingly to elemental analysis.

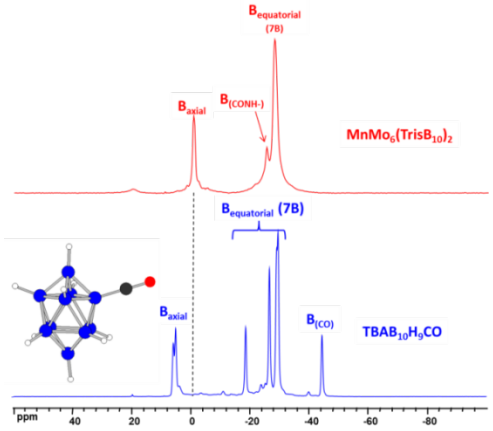

Figure 2*: $^{11}B\{^1H\}$ NMR spectra comparing $TBAB_{10}H_9CO$, and $MnMo_6(TRIS\text{-}B_{10})_2$*

In addition to the peaks of TBA^+ and solvents, the ^1H and the $^1H\{^{11}B\}$ NMR spectra of **$MnMo_6(TRIS\text{-}B_{10})_2$** (Figures 3 and S12) and of **$AlMo_6(TRIS\text{-}B_{10})$** (Figures S9-S10, ESI) display additional signals assigned to $DIPEAH^+$ found as secondary countercations and a small new broad peak, at 6.2 ppm or at 6.8 ppm respectively, attributed to the formation an amide function,[7] accordingly to the expected grafting of boron cluster on the tris-Anderson POMs. The ^1H and $^1H\{^{11}B\}$ NMR spectra of **$AlMo_6(TRIS)$** recorded in CD_3CN (Figures S9-S10, ESI) display two peaks of relative integration 6:3, at 4.6 and 4.0 ppm which are respectively assigned to the methylene groups of the Tris ligands and to the 3 OH groups linked to the Al center.[20] Upon reaction with TBA[$B_{10}H_9CO$], the signal of OH groups is not affected, while the signal of the methylene groups of the TRIS ligand appears as a multiplet in the 4.3-4.8 ppm range, suggesting that the

rotation of the amide function is blocked by energy barrier,[25] which translates by the nonequivalence of the three methylene groups of the TRIS ligand. Besides, a shoulder corresponding to a minor proportion of the starting compound **$AlMo_6$(TRIS)** is also observed. For **$MnMo_6$(TRIS)$_2$**, due to their proximity to the Mn^{III} center, the singlet attributed to the three equivalent methylene groups of the TRIS ligands appears strongly unshielded at 60.7 ppm.[19, 23] In **$MnMo_6$(TRIS-B_{10})$_2$**, this signal is slightly shifted upfield and split into at least four components in the range 61-64 ppm. This result originates from the formation of the amide blocked in a configuration in which the methylene groups of the TRIS ligands are not equivalent, as observed previously with **$AlMo_6$(TRIS-B_{10})**. Finally, for both compounds the equatorial B-H groups of the boron cluster are well seen in the $^1H\{^{11}B\}$ NMR spectra (Figures S9 and S12, ESI) at 0.2 and 0.4 ppm and appear significantly shifted from those observed in the precursor TBA($B_{10}H_9CO$) (0.7 and 0.4 ppm respectively), while the signals of apical B-H groups can hardly be distinguished overlapping with other signals.

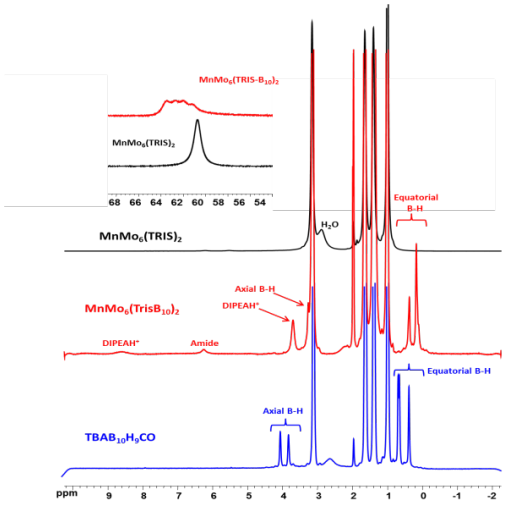

Figure 3: *^1H NMR spectra of $MnMo_6$(TRIS)$_2$, TBA[$B_{10}H_9CO$], and $MnMo_6$(TRIS-B_{10})$_2$ compounds*

Absorption spectroscopy was used to probe the electronic consequences of covalent decahydroborate–POM linkage (Figure S13-S14, ESI). The electronic spectra of compounds **$AlMo_6$(TRIS-B_{10})** and **$MnMo_6$(TRIS-B_{10})$_2$** recorded in CH_3CN are dominated by strong absorption bands in UV region corresponding to the LMCT transition between p-orbitals of the oxo ligands and d-type orbitals centered on molybdenum,[26] while the cluster $[B_{10}H_9CO]^-$ exhibits weak absorption band between 300 and 200 nm notably assigned to π-π^* transitions. The electronic spectra of the two adducts **$AlMo_6$(TRIS-B_{10})** and **$MnMo_6$(TRIS-B_{10})$_2$** differs significantly from the spectra of their parent precursors in terms of intensities of the absorption bands, while the positions of their maxima appears very similar. These observations suggest significant electronic coupling between the boron clusters and the Anderson entities, which were investigated by electrochemistry. The cyclic voltamograms (CVs) recorded for $MnMo_6$(TRIS)$_2$ and **$MnMo_6$(TRIS-B_{10})$_2$** in dry CH_3CN in the presence of $TBAClO_4$ as supporting electrolyte are given in Figure 4 and in ESI (Figures S15-S17). The CV of the precursor $MnMo_6$(TRIS)$_2$ displays a one-electron reversible wave in oxidation centered at E_p = + 410 mV *vs.* Fc^+/Fc (ΔEp = 145 mV at v = 100 mV.s^{-1}) assigned to the oxidation of the Mn^{III} center of the Anderson POM into Mn^{IV},[23, 27, 28] while a one electron reduction wave is observed at Ep = -1090 mV *vs.* Fc^+/Fc (ΔEp = 320 mV at v = 100 mV.s^{-1}) This process, separated by ΔE = 320 mV, is also mono-electronic and corresponds to the reduction of Mn^{III} into Mn^{II} as demonstrated in literature.[27] The reduction of Mo^{VI} centers is observed at lower potential but this process is usually irreversible.[29] In similar conditions the CV of **$MnMo_6$(TRIS-B_{10})$_2$** demonstrates that the grafting of the B_{10} clusters on $MnMo_6$(TRIS)$_2$ influences on the electronic properties of the Mn^{III} center. It provokes a shift of 90 mV of the Mn^{IV}/Mn^{III} wave in the negative direction to E_p = + 320 mV vs. Fc^+/Fc with the loss of the reversibility, while the reduction of Mn^{III} into Mn^{II} occurs at -1712 mV vs. Fc^+/Fc and is significantly shifted by around 450 mV towards the more negative values of potential compared to its precursor $MnMo_6$(TRIS)$_2$. The reoxidation process occurs at E_{pa} = -1118 mV vs Fc^+/Fc, thus giving a very large difference of potential and thus a very slow process. These significant modifications are in agreement with the increase of the negative charge from 3- in $MnMo_6$(TRIS)$_2$ to 7- in **$MnMo_6$(TRIS-B_{10})$_2$** and also in agreement with the grafting of two electron-donating boron clusters,[30] which increases the electronic density at the Mn^{III} center of the POM and hence should destabilize the reduced state of the POMs. Finally, some partial degradation both in oxidation and reduction is observed by cycling several times (see ESI).

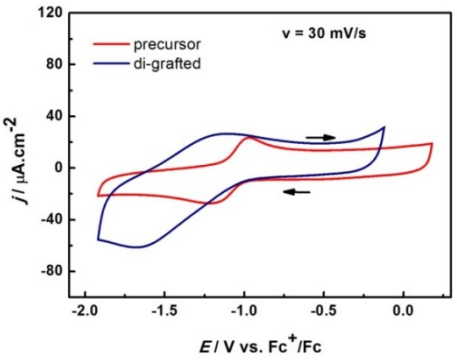

Figure 4: *Cyclic voltamograms (CVs) of $MnMo_6$(TRIS)$_2$ and **$MnMo_6$(TRIS-B_{10})$_2$** in the reduction part at a scan rate of 30 mV.s^{-1}. The concentrations of compounds are 2.10^{-4} M; the electrolyte was ACN + 0.1M $TBAClO_4$.*

Analysis of the electronic structure of the Mn derivatives showed that both the HOMO and LUMO orbitals are Mn-centred, which both shift up by 0.1 eV upon **B_{10}** addition (Figure S19, ESI). The mixing between POM and **B_{10}** orbitals is practically non-existent, and the H/L gap is kept constant. The computed UV/Vis spectra (Figure S20) shows good agreement with the experiment. The increase of energy in the LUMO is related to the increase in the reduction potential of Mn^{III} to Mn^{II}, while the increase in the HOMO fits to easier oxidation to Mn^{IV}.

Finally, we evaluated the relative stability of the boron products with respect their respective reactants. Since the coupling between the amine in the POM and the carbonyl group in the borane release the product plus proton, direct evaluation of the reaction energy for the formation of

$AlMo_6(TRIS\text{-}B_{10})$ and **$MnMo_6(TRIS\text{-}B_{10})_2$** from their TRIS counterparts was straightforward. Figure 5 depicts the free energy profile for the formation of product **$AlMo_6(TRIS\text{-}B_{10})$** and of **$MnMo_6(TRIS\text{-}B_{10})_2$** together with intermediate **$MnMo_6(TRIS\text{-}B_{10})$**. These energies suggest that the lack of total conversion in **$AlMo_6(TRIS\text{-}B_{10})$** relies on the isoergonic character of the reaction, since there is any gain in stability in the product. On the other side, formation of the Mn derivatives **$MnMo_6(TRIS\text{-}B_{10})$** and **$MnMo_6(TRIS\text{-}B_{10})_2$** is clearly more favourable.

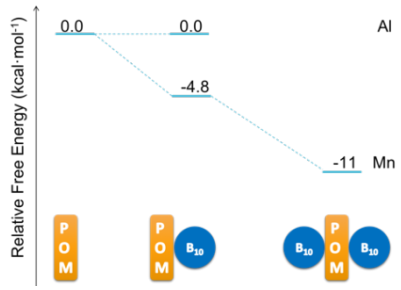

Figure 5: *Free energy reaction profile of* ***$AlMo_6(TRIS\text{-}B_{10})$*** *and* ***$MnMo_6(TRIS\text{-}B_{10})_2$*** *formation.*

Conclusions

We succeeded in associating one or two anionic closo-decahydrodecaborate cluster to anionic Al and Mn-Anderson POMs functionalized by TRIS ligands through the formation of amide bond between the two entities. The two novel adducts were characterized by FT-IR, ESI-MS, NMR, UV-Visible spectroscopy and electrochemistry. IR and UV properties derived from molecular structures obtained by means of DFT methods are in full agreement with experimental data and evidenced the electronic effects resulting from this combination. In particular, it demonstrated the athermic character of the formation of the adduct with Al-Anderson POM while the formation of Mn analogue is exothermic. These compounds constitute a unique association of these two classes of compounds but the marriage of these two entities remains fragile and the decomposition of the adducts by heating or by oxidation appears relatively easy. These two topics are currently under study in our group to improve the stability of such compounds.

Acknowledgements

Ms Cladeen Boukama is acknowledged for her contribution to the electrochemical studies. This work is supported by a public grant overseen by the French National Research Agency (ANR) as part of the « Investissements d'Avenir » program (Labex Charm3at, ANR-11-LABX-0039-grat). MD thanks AZM association and IUF for financial support. We also thank CERCA Program and AGAUR (2017SGR00290) of the Generalitat de Catalunya, and the Spanish Ministerio de Cienci, Innovación y Universidades through project TQ2017-88777-R. International collaboration supported by IRN-CNRS 2019-2023.

Conflicts of interest

There are no conflicts to declare.

Notes and references

1. Y. Zhu and N. S. Hosmane, *Coord. Chem. Rev.*, 2015, **293**, 357-367.
2. N. S. Hosmane, *Boron Science: New Technologies and Applications*, CRC Press, 2012.
3. Y. Zhu and N. S. Hosmane, *Pure Appl. Chem.*, 2018, **90**, 653-663.
4. E. Hey-Hawkins and C. Viñas-Teixidor, *Boron-Based Compounds: Potential and Emerging Applications in Medicine*, John Wiley&sons Ltd, 2018.
5. I. B. Sivaev, A. V. Prikaznov and D. Naoufal, *Collect. Czech. Chem. Commun.*, 2010, **75**, 1149-1199.
6. F. Abi-Ghaida, S. Clement, A. Safa, D. Naoufal and A. Mehdi, *J. Nanomater.*, 2015, Article Number: 608432
7. F. Abi-Ghaida, Z. Laila, G. Ibrahim, D. Naoufal and A. Mehdi, *Dalton Trans.*, 2014, **43**, 13087-13095.
8. T. Yamase, *J. Mater. Chem.*, 2005, **15**, 4773-4782.
9. B. Hasenknopf, *Front. Biosci.*, 2005, **10**, 275-287.
10. A. Bijelic, M. Aureliano and A. Rompel, *Angew. Chem.-Int. Edit.*, 2019, **58**, 2980-2999.
11. N. I. Gumerova, E. Al-Sayed, L. Krivosudsky, H. Cipic-Paljetak, D. Verbanac and A. Rompel, *Frontiers in Chemistry*, 2018, **6**.
12. G. Izzet, F. Volatron and A. Proust, *Chem. Rec.*, 2017, **17**, 250-266.
13. A. Proust, B. Matt, R. Villanneau, G. Guillemot, P. Gouzerh and G. Izzet, *Chem. Soc. Rev.*, 2012, **41**, 7605-7622.
14. A. Dolbecq, E. Dumas, C. R. Mayer and P. Mialane, *Chem. Rev.*, 2010, **110**, 6009-6048.
15. A. Blazevic and A. Rompel, *Coord. Chem. Rev.*, 2016, **307**, 42-64.
16. C. Yvon, A. Macdonell, S. Buchwald, A. J. Surman, N. Follet, J. Alex, D. L. Long and L. Cronin, *Chem. Sci.*, 2013, **4**, 3810-3817.
17. E. Al-Sayed, A. Blazevic, A. Roller and A. Rompel, *Chem.-Eur. J.*, 2015, **21**, 17800-17807.
18. A. Blazevic, E. Al-Sayed, A. Roller, G. Giester and A. Rompel, *Chem.-Eur. J.*, 2015, **21**, 4762-4771.
19. H. Karoui and C. Ritchie, *Dalton Trans.*, 2016, **45**, 18838-18841.
20. H. Ai, Y. Wang, B. Li and L. Wu, *Eur. J. Inorg. Chem.*, 2014, 2766-2772.
21. P. R. Marcoux, B. Hasenknopf, J. Vaissermann and P. Gouzerh, *Eur. J. Inorg. Chem.*, 2003, 2406-2412.
22. K. Shelly, C. B. Knobler and M. F. Hawthorne, *Inorg. Chem.*, 1992, **31**, 2889-2892.
23. O. Oms, K. Hakouk, R. Dessapt, P. Deniard, S. Jobic, A. Dolbecq, T. Palacin, L. Nadjo, B. Keita, J. Marrot and P. Mialane, *Chem. Commun.*, 2012, **48**, 12103-12105.
24. E. S. Shubina, E. V. Bakhmutova, A. M. Filin, I. B. Sivaev, L. N. Teplitskaya, A. L. Chistyakov, I. V. Stankevich, V. I. Bakhmutov, V. I. Bregadze and L. M. Epstein, *J. Organomet. Chem.*, 2002, **657**, 155-162.
25. T. Le Borgne, J. M. Benech, S. Floquet, G. Bernardinelli, C. Aliprandini, P. Bettens and C. Piguet, *Dalton Trans.*, 2003, 3856-3868.
26. K. Hakouk, O. Oms, A. Dolbecq, J. Marrot, A. Saad, P. Mialane, H. El Bekkachi, S. Jobic, P. Deniard and R. Dessapt, *J. Mater. Chem. C*, 2014, **2**, 1628-1641.
27. S. Schoenweiz, M. Heiland, M. Anjass, T. Jacob, S. Rau and C. Streb, *Chem.-Eur. J.*, 2017, **23**, 15370-15376.
28. S. Schonweiz, S. A. Rommel, J. Kubel, M. Micheel, B. Dietzek, S. Rau and C. Streb, *Chem.-Eur. J.*, 2016, **22**, 12002-12005.
29. M. T. Pope, *Heteropoly and Isopoly Oxometalates*, Springer-Verlag, Berlin, 1983.

30. I. B. Sivaev, A. V. Prikaznov and S. A. Anufriev, *J. Organomet. Chem.*, 2013, **747**, 254-256.